



UDC 669.15-194.55:539.374

DOI 10.17073/0368-0797-2025-1-21-29



Оригинальная статья
Original article

TENSILE FRACTURE OF TEMPERED MARTENSITIC STEEL

L. A. Tepliyakova¹, T. S. Kunitsyna¹, V. A. Pechkovskii¹, A. D. Kashin²

¹ Tomsk State University of Architecture and Building (2 Solyanaya Sqr., Tomsk 634003, Russian Federation)

² Institute of Strength Physics and Materials Science, Siberian Branch of the Russian Academy of Sciences (2/4 Akademicheskii Ave., Tomsk 634055, Russian Federation)

✉ lat168@mail.ru

Abstract. The work is devoted to the study of development regularities of plastic deformation and destruction of medium-alloy steel with a tempered martensite structure (0.34C–Cr–Ni–3Mo–V–Fe steel) under active tension. This steel is characterized by a multi-scale defect structure and contains cementite precipitates and special carbides. An experimental study of the evolution of defect and carbide subsystems during plastic deformation required the use of different methods: optical and electron (scanning and transmission) microscopy; X-ray structural analysis; measurements of quantitative characteristics of the microstructure and pattern of microcracks and their statistical processing. The research revealed that the places of significant localization of plastic deformation at the pre-destruction stage are the boundary areas of grains (former austenitic and real martensitic); all structural components of tempered martensite (plates, packets, blocks of laths, laths). A comparison of nature of the deformation relief and the fine structure formed before destruction with the pattern of fractures at various structural-scale levels indicates that the destruction of the steel under study, as well as the plastic deformation preceding it, bears the features of heredity of the original internal structure. Thus, the fracture of the studied steel has a multi-level nature, caused by: hierarchy of the initial internal microstructure; evolution of carbide phases; localization of plastic deformation developing at all stages of plastic deformation and, as a consequence, preparing the paths for microcracks propagation.

Keywords: tempered lath martensite, dislocation structure, deformation relief, fracture surface, scale-structural levels of fracture

For citation: Tepliyakova L.A., Kunitsyna T.S., Pechkovskii V.A., Kashin A.D. Tensile fracture of tempered martensitic steel. *Izvestiya. Ferrous Metallurgy*. 2025;68(1):21–29. <https://doi.org/10.17073/0368-0797-2025-1-21-29>

РАЗРУШЕНИЕ ОТПУЩЕННОЙ МАРТЕНСИТНОЙ СТАЛИ ПРИ РАСТЯЖЕНИИ

Л. А. Теплякова¹, Т. С. Куницына¹, В. А. Печковский¹, А. Д. Кашин²

¹ Томский государственный архитектурно-строительный университет (Россия, 634003, Томск, пл. Соляная, 2)

² Институт физики прочности и материаловедения Сибирского Отделения РАН (Россия, 634055, Томск, пр. Академический, 2/4)

✉ lat168@mail.ru

Аннотация. Настоящая работа посвящена изучению закономерностей развития пластической деформации и разрушения среднелегированной стали со структурой отпущенного мартенсита (сталь 34ХНЗМФА) при активном растяжении. Данная сталь отличается многомасштабной дефектной структурой и содержит выделения цементита и специальные карбиды. Экспериментальное исследование эволюции дефектной и карбидной подсистем при пластической деформации потребовало применения комплекса методов: оптическая и электронная (сканирующая и просвечивающая) микроскопия, рентгеноструктурный анализ; измерения количественных характеристик микроструктуры и картины микротрещин и их статистическая обработка. В работе выявлено, что местами существенной локализации пластической деформации на стадии предразрушения являются приграничные области: зерен (бывшего аустенитного и реального мартенситного); всех структурных составляющих отпущенного мартенсита (пластины, пакеты, блоки реек, рейки). Сопоставление характера деформационного рельефа и тонкой структуры, формирующейся перед разрушением, с картиной изломов на различных структурно-масштабных уровнях свидетельствует о том, что разрушение исследованной стали, также как и пластическая деформация, ей предшествующая, несет в себе черты наследственности исходной внутренней структуры. Таким образом, разрушение исследованной стали имеет многоуровневый характер, обусловленный: иерархией исходной внутренней микроструктуры; эволюцией карбидных фаз; локализацией пластической деформации, развивающейся на всех стадиях пластической деформации и, как следствие, подготавливающей пути распространения микротрещин.

Ключевые слова: пакетный отпущенный мартенсит, дислокационная структура, деформационный рельеф, поверхность разрушения, масштабно-структурные уровни разрушения

Для цитирования: Теплякова Л.А., Куницына Т.С., Печковский В.А., Кашин А.Д. Разрушение отпущенной мартенситной стали при растяжении. *Известия вузов. Черная металлургия.* 2025;68(1):21–29. <https://doi.org/10.17073/0368-0797-2025-1-21-29>

INTRODUCTION

Steel with a tempered martensite structure exhibits good plastic properties combined with high strength both at the initial stages of deformation [1 – 3] and under significant degrees of plastic deformation [4 – 6]. The optimal mechanical properties of martensitic steel are the reason for its wide industrial application [7], particularly in the automotive industry [8]. It is known that the internal structure of steel with a tempered martensite structure is hierarchically organized within a range of scales differing by three orders of magnitude [8 – 11]. The main morphological component of martensite is tempered lath martensite [9; 10]. The basic element of this microstructure is a lath with a width ranging from 0.2 to 0.5 μm . Laths tend to align parallel to each other within large regions of the parent austenitic grain in which they form. A group of laths with the same orientation is referred to as a block, and a group of several blocks sharing the same habit plane is called a packet. The boundaries of both blocks and packets are effective barriers to dislocation motion, providing the strength and impact toughness of martensitic steels [2; 3]. It should be noted that the mechanisms of plastic deformation in steels with such a complex defect structure are still insufficiently studied [7; 12]. Previous studies [13; 14] have shown that for medium-alloy steel with a tempered martensite structure under active tension, there is pronounced localization of deformation associated with the boundaries of misorientation between inherited austenitic grains and real martensitic grains. These studies revealed that during active loading, plastic deformation undergoes self-organization within groups of real grains. The linear dimensions of martensitic grain groups that self-organize during deformation are comparable to the sizes of the inherited austenitic grains. In other words, during plastic deformation, deformation localization occurs in close relation to the grain subsystem.

The development of shear deformation in the packet component of martensite is also accompanied by shear localization, which is related to the hierarchical structure of packet martensite. In [15], it was established that within packets of martensitic crystals (laths), localization occurs through the formation of two subsystems of shear traces: fine and coarse. The fine shear trace subsystem forms from the very beginning of plastic deformation under conditions of homogeneous sample deformation. The emergence and evolution of the coarse shear trace subsystem correlate with the formation of the first

(elongated) neck in the sample, representing the main micromechanism leading to the localization of plastic deformation at the sample scale (macrolocalization). The sites of coarse shear localization are the boundary areas of laths and packet fragments. The appearance of coarse shear trace subsystems correlates with the formation of a fragmented (isotropic) dislocation structure within the packet. In other words, shear plastic deformation in steel with a tempered martensite structure is closely linked to its hierarchically organized localization throughout all stages of deformation, including those preceding fracture. According to the results of these studies, it is logical to assume that the fracture of this class of steel should also be hierarchically conditioned by the preceding deformation.

The present study aims to establish the development regularities of the fracture process in medium-alloy steel with a tempered martensite structure within a physically justified range of scales and to identify its relation to the preceding plastic deformation.

MATERIAL AND METHODS

For this study, 0.34C–Cr–Ni–3Mo–V–Fe steel was used. Following rolling, the steel underwent quenching from 950 °C in water, followed by tempering at 600 °C for 4 h and subsequent water cooling as the final stage of heat treatment. After thermomechanical processing, the steel developed a structure of highly tempered mixed packet-lath martensite. Most of the carbon is present in the form of carbide precipitates, including cementite and special carbides, predominantly Me_2C , Me_6C and Me_{23}C . Tensile testing was performed on an Instron machine at a strain rate of $6 \cdot 10^{-4} \text{ s}^{-1}$ at room temperature. The fracture surface was analyzed using optical microscopy, scanning electron microscopy (SEM), and transmission electron microscopy (TEM) on samples cut parallel and perpendicular to the rolling direction, referred to as longitudinal and transverse samples, respectively. Measurements were taken for the microcrack density, their length, and the orientation angles relative to the tensile axis. The measurement results were subjected to statistical processing, and the corresponding average values were determined.

RESEARCH RESULTS AND DISCUSSION

Initial structure (before deformation). The internal structure of the studied 0.34C–Cr–Ni–3Mo–V–Fe steel before loading represents a complex system.

It includes: boundaries of misorientation between grains and all structural components of martensite (plates, packets, packet fragments – blocks, and laths); a developed dislocation structure with an average scalar dislocation density of approximately 10^{10} cm^{-2} ; a subsystem of carbide phases, consisting of cementite and special carbides. The structural and phase analyses conducted in this study, combined with the assessment of quantitative characteristics, made it possible to create, in effect, a “passport” for the investigated steel. This passport provides a detailed representation of the hierarchical organization of the internal structure across the entire physically justified range of scales. The results of this analysis are summarized in Table 1. The dislocation structure within packets and plates is diverse, including network, cellular, and fragmented substructures [1; 16]. Cementite precipitates are predominantly located along the boundaries of martensitic structural components, while the distribution of special carbides is closely associated with the dislocation substructure. In the network structure, special carbides are found at the nodes of dislocation networks, whereas in the cellular and fragmented substructures,

they are located at the junctions of cell boundaries and fragment interfaces, respectively [11; 16].

During plastic deformation, both the defect and carbide subsystems undergo significant evolution, accompanied by multi-level deformation localization [13 – 15] and transformations of carbide phases [17]. In steel with a tempered martensite structure, crack initiation is generally not a critical concern. However, potential sites for microcrack initiation include non-metallic inclusions, various misorientation boundaries and their intersections, as well as carbide particles. Understanding the conditions that enable initiated cracks to propagate is therefore of great importance. It is noteworthy that most of the current knowledge regarding the structure of microcracks and the fracture surface has been obtained using optical microscopy and scanning electron microscopy [18 – 21]. In contrast, the application of transmission electron microscopy on foils remains relatively uncommon in studies of fracture processes [22; 23].

In this study, an extensive electron microscopy investigation was conducted to examine

Table 1. Classification of structural levels by scale

Таблица 1. Классификация структурных уровней по масштабу

Scale level number	Structural level number	Structural element		Average size, μm
1	1	Entire sample		$(4 \times 4 \times 6) \cdot 1000$
2	2	Segregation bands		50×5000
	3	Non-metallic inclusions (sulfides)		20×30
	4	Inherited grain (group of real grains)		140
	5	Real grain		20
3	6	Packet		4×6
	7	Plate		2.5×4.0
	8	Packet fragment (block)		0.8×4.0
4	9	Packet martensite crystal (lath)		0.19×4.0
	10	Lath fragment		0.6×4.0
5	11	Cementite particles	At plate boundaries	$(0.6 \times 4) \cdot 10^{-2}$
			At lath boundaries	$(3 \times 25) \cdot 10^{-2}$
			In plate matrix	$(2 \times 14) \cdot 10^{-2}$
			In lath matrix	$(1.7 \times 10) \cdot 10^{-2}$
	12	Special carbide particles	At plate boundaries	$8 \cdot 10^{-2}$
			At lath boundaries	$1.6 \cdot 10^{-2}$
			In plate matrix	$1.1 \cdot 10^{-2}$
			In lath matrix	$1.4 \cdot 10^{-2}$
13	Dislocation cell		$4 \cdot 10^{-2} - 5 \cdot 10^{-2}$	
14	Dislocation cell link		$1 \cdot 10^{-2} - 15 \cdot 10^{-2}$	

the fine structure at various stages of plastic flow in 0.34C–Cr–Ni–3Mo–V–Fe steel, covering deformation levels up to those preceding fracture (in the region of the second neck [13]).

Microcracks and interface boundaries. Fig. 1 presents typical examples of the fine structure of the steel, highlighting microcracks propagating along interface boundaries. These boundaries were formed both as a result of prior thermomechanical treatment – including grain boundaries (Fig. 1, *a*), the boundaries of martensitic structural components such as packets and plates (Figs. 1, *b, c*), and lath boundaries (Fig. 1, *d*) – as well as along boundaries of dislocation fragments generated during plastic deformation (Figs. 1, *e, f*).

Analysis of numerous micrographs obtained in this study reveals that microcracks tend to propagate along surfaces where highly localized shear deformation has occurred. This phenomenon represents the natural outcome of localized deformation, arising from the insufficient relaxation of internal stresses through mechanisms other than microcrack formation. This observation is consistent with the fact that, in steel with a tempered martensite structure, local stress concentrations in specific regions can reach values comparable to the material’s theoretical strength, even though the average stress levels correspond to the actual ultimate strength, typically achieved during the later stages of plastic deformation [16]. Moreover, it is noteworthy that microcrack

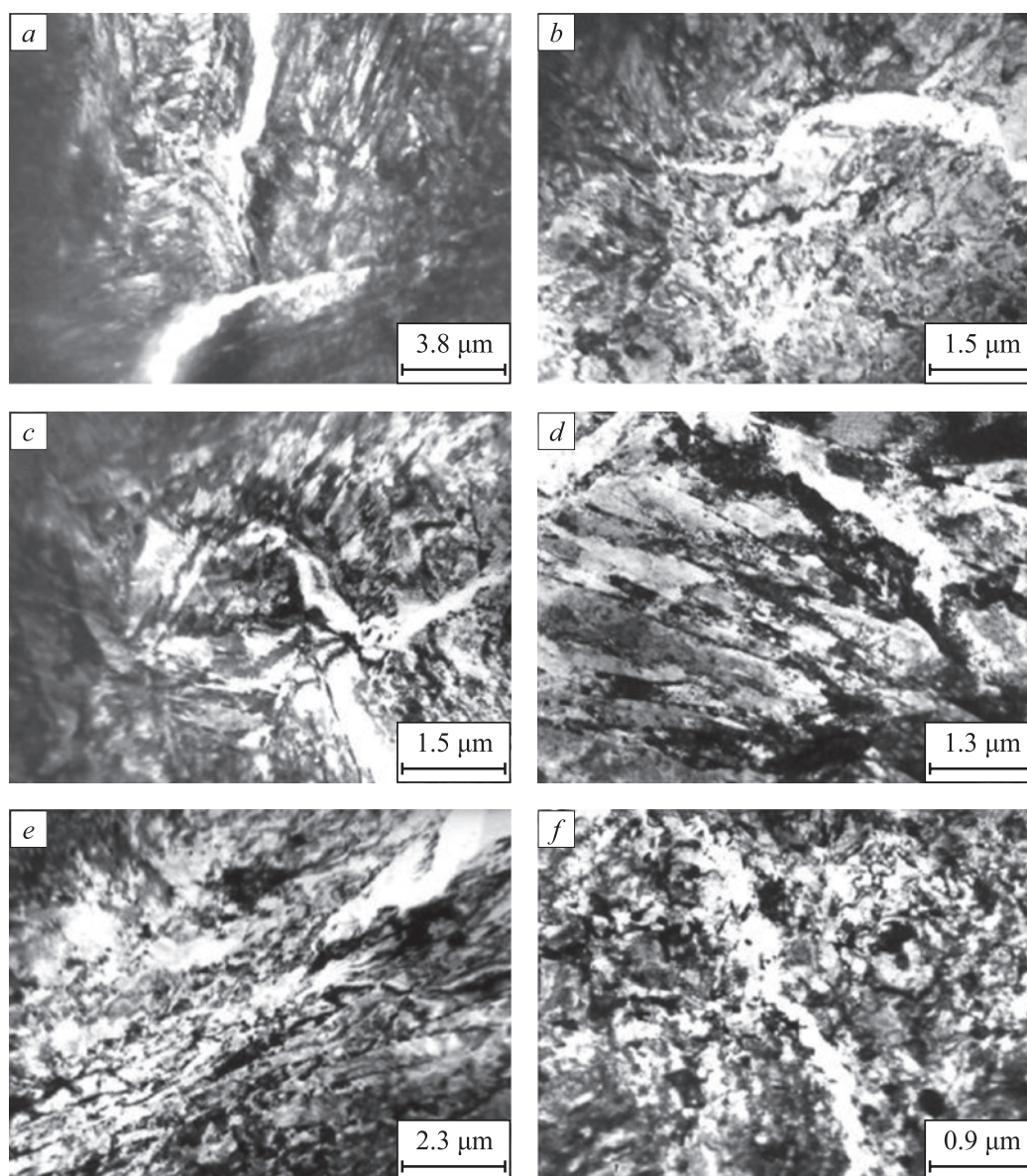


Fig. 1. Cracks propagating along grain boundaries (*a, b*), structural components of martensite (*c, d*) and fragments (*e, f*)

Рис. 1. Трещины, распространяющиеся по границам зерен (*a, b*), структурных составляющих мартенсита (*c, d*) и фрагментов (*e, f*)

propagation paths frequently pass through regions characterized by an isotropic fragmented substructure. This substructure represents the final stage in the sequence of substructural transformations observed in this steel, progressing from network to cellular, then to anisotropic fragments, and finally to the isotropic fragmented substructure [24]. This sequence of transformations occurs earlier at interface boundaries than in the surrounding matrix, indicating that these boundary regions exhaust their available mechanisms for relaxing localized long-range stress amplitudes – induced during deformation – sooner than the matrix itself.

Microcracks. In the studied steel with a mixed tempered martensite structure, which contains a subsystem of sub-boundaries formed during thermomechanical treatment, microcracks appear from the very onset of plastic deformation. As noted earlier, deformation leads to the formation of new misorientation boundaries (boundaries of dislocation fragments within martensite crystals), with their misorientation angles increasing

as the degree of deformation grows [17; 24]. Simultaneously, there is an increase in the microcrack density and a decrease in their average length (Fig. 2, a), which correlates with the rising overall density of misorientation boundaries in martensite and their intersections.

The average length of microcracks prior to fracture is approximately 1 μm, which is comparable to the typical linear dimensions of a lath block (Table 1). This indicates that microcracks in this steel cross lath boundaries but are impeded by block boundaries, which exhibit larger misorientation angles than lath boundaries [14; 19].

In this study, the proportions of microcracks oriented at various angles relative to the tensile axis were measured, and the results are presented in Fig. 2, b. At higher degrees of deformation, microcracks oriented at 45° to the tensile axis become predominant, while the proportion of cracks oriented parallel to the tensile axis decreases significantly. This indicates the dominance of cleavage cracks at advanced deformation stages [22].

Scale-structural levels of fracture. As previously discussed, the internal structure of steel with a tempered martensite structure consists of three hierarchically organized subsystems: misorientation boundaries, a developed dislocation structure, and carbide phase precipitates. During plastic deformation, each of these subsystems evolves within its corresponding scale range, with their evolutionary patterns being interconnected and mutually dependent (for more details, see [17; 24]). Given this hierarchical organization, it was expected that the ductile fracture of this steel would also display a multi-level character. In this study, the fracture surfaces of the samples were examined across a range of scales differing by three orders of magnitude. Table 2 presents micrographs alongside quantitative characteristics of the fracture patterns observed in both longitudinal and transverse samples of 0.34C–Cr–Ni–3Mo–V–Fe steel with a tempered martensite structure, reflecting distinct structural scale levels.

The longitudinal samples predominantly exhibit a cup-and-cone fracture, whereas the transverse samples display a combination of cup-and-cone and brittle fracture features. The linear dimensions of the dimples at various scale levels were measured, their average values determined, and these measurements were compared with the average sizes of structural elements listed in Table 1. This comparison revealed a clear correlation between the fracture surface characteristics and the average sizes of key structural components, including inherited grains, real grains, plates, packets, and finer elements such as dislocation fragments formed during plastic deformation at strain levels preceding fracture (Table 1, Level 4). The identified correlation is consistent with previously established patterns [13 – 15] of multi-level, hierarchically organized localization of plastic deformation

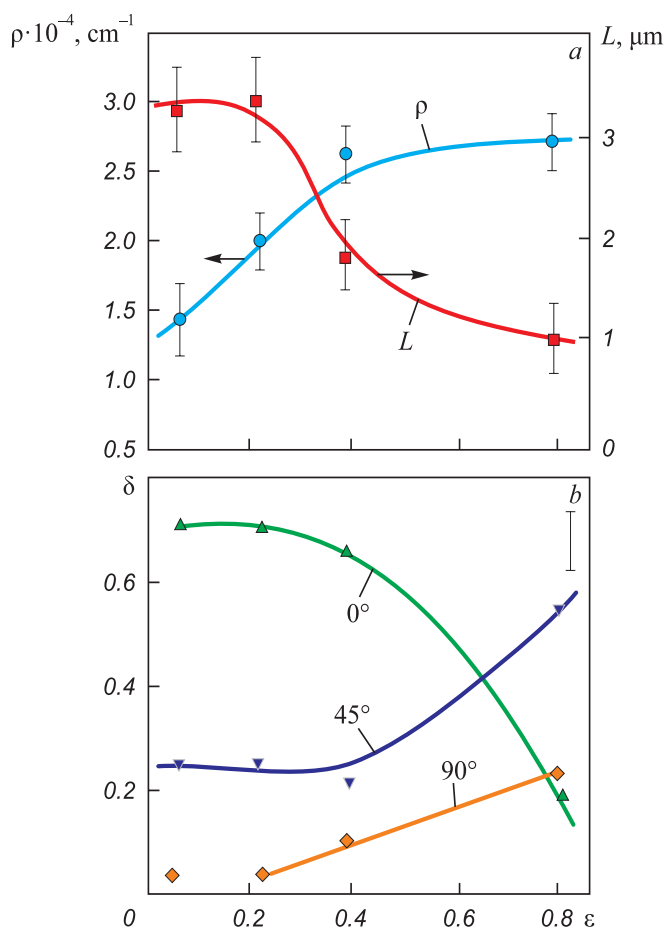
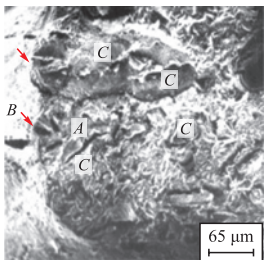
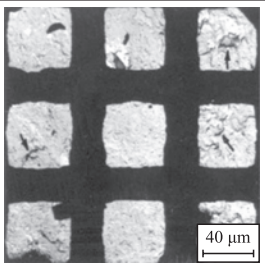
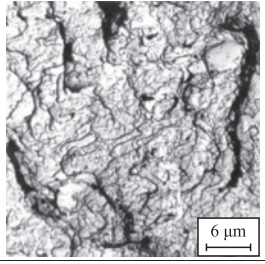
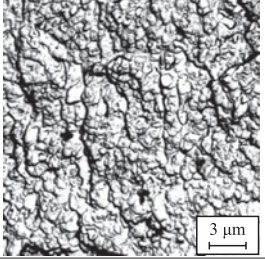
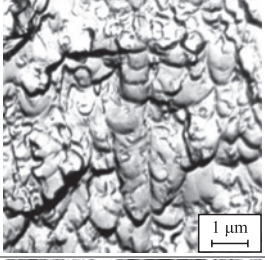
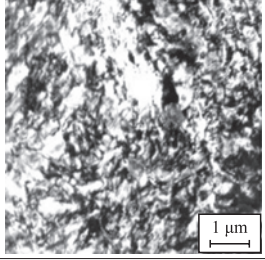


Fig. 2. Relationship between crack density ρ , their length L (a) and proportion of cracks δ parallel (0°), perpendicular (90°) and running at an angle of 45° to the tensile axis (b) with deformation degree

Рис. 2. Связь плотности трещин ρ , их длины L (a) и доли трещин δ , параллельных (0°), перпендикулярных (90°) и идущих под углом 45° к оси растяжения (b) со степенью деформации

Table 2. Characteristics of the fracture pattern

Таблица 2. Характеристики картины изломов

Structural-scale level	Observed fracture feature	Micrograph of the fracture feature	Characteristic size of the fracture feature, μm	Average spacing between fracture features, μm	Corresponding microstructural element
Entire sample (Level 1)	Cracks (A) Pits (B) Quasi-brittle fracture zones (C)		Average crack length ~150 Pit diameter 50 – 100 Quasi-brittle zone diameter 200 – 500	~100	Grain groups. Non-metallic inclusions
Grain group (Level 2)	Bands of localized plastic deformation		Band width 0.5 – 1.5	50 – 300	Result of plastic deformation near grain boundaries
					
Grain (Level 3)	Bands of localized deformation Regions with uniform dimple morphology Dimples within these regions Elongated dimples		Band width ~0.3	6,5	Packet groups
			6×10	6×10	Packets
			0.64	0.56	Lath or lath groups within packets
			1.5×9.0	–	Plates
Packet, plate (Level 4)	Internal structure of dimples		0.5 – 0.6		Fragments within laths and plates
	Fragmented substructure		Fragment size: In plates – 0.35×0.08 in laths – 0.18×0.07		

tion along misorientation boundaries. Notably, as shown in [15], the average shear intensity in the boundary regions of tempered martensite crystals (blocks and laths) is approximately three times higher than in the crystal matrix. In other words, the intense localization of plastic deformation facilitates the formation of preferential pathways for microcrack propagation.

In conclusion, the comparison of the deformation relief and the fine structure formed prior to fracture with the fracture patterns observed at different structural-scale levels demonstrates that the fracture of the studied steel, much like the plastic deformation that precedes it, reflects the inherited characteristics of the original internal structure.

CONCLUSIONS

The initiation and propagation of microcracks in steel with a tempered martensite structure at the later stages of plastic deformation were investigated using various analytical methods. The results showed that almost all observed microcracks propagate along interface boundaries, specifically: grain boundaries and the boundaries of coherently deforming grain groups, the boundaries of plates, packets, and lath blocks, and the boundaries of dislocation substructure fragments, which represent the final stage in the sequence of substructural transformations in the studied steel.

It was found that during plastic deformation, the length of microcracks decreases, and in the deformation stage preceding fracture, microcracks can cross lath boundaries but are typically arrested at block boundaries. Notably, the majority of these microcracks form through the cleavage mechanism.

The fracture process in the studied steel exhibits a multi-level nature, determined by: the hierarchical structure of the original internal microstructure, the localization of plastic deformation, which evolves throughout all stages of plastic deformation, and, as a result, the formation of preferential pathways for microcrack propagation.

REFERENCES / СПИСОК ЛИТЕРАТУРЫ

- Ivanov Yu.F., Gromov V.E., Popova N.A., Konovalov S.V., Koneva N.A. Structural and Phase States and Mechanisms of Hardening of Deformed Steel. Novokuznetsk: Polygraphist; 2016:510. (In Russ.).
Структурно-фазовые состояния и механизмы упрочнения деформированной стали / Ю.Ф. Иванов, В.Е. Громов, Н.А. Попова, С.В. Коновалов, Н.А. Конева. Новокузнецк: Полиграфист; 2016:510.
- Harjo S., Kawasaki T., Tomota Y., Gong W., Aizawa K., Tichy G., Shi Z., Ungár T. Work hardening, dislocation structure, and load partitioning in lath martensite determined by in situ neutron diffraction line profile analysis. *Metallurgical and Materials Transactions A*. 2017;48(9):4080–4092. <https://doi.org/10.1007/s11661-017-4172-0>
- Kwak K., Mayama T., Mine Y., Takashima K. Anisotropy of strength and plasticity in lath martensite steel. *Materials Science and Engineering: A*. 2016;674:104–116. <https://doi.org/10.1016/j.msea.2016.07.047>
- Jo K.-R., Seo E.-J., Sulistiyo D.H., Kim J.-K., Kim S.-W., De Cooman B.C. On the plasticity mechanisms of lath martensitic steel. *Materials Science and Engineering: A*. 2017;704:252–261. <https://doi.org/10.1016/j.msea.2017.08.024>
- Jafarian H.R., Tarazkouhi M.F. Significant enhancement of tensile properties through combination of severe plastic deformation and reverse transformation in an ultrafine/nano grain lath martensitic steel. *Materials Science and Engineering: A*. 2017;686:113–120. <https://doi.org/10.1016/j.msea.2017.01.034>
- Shamsujjoha M. Evolution of microstructures, dislocation density and arrangement during deformation of low carbon lath martensitic steels. *Materials Science and Engineering: A*. 2020;776:139039. <https://doi.org/10.1016/j.msea.2020.139039>
- Inoue J., Sadeghi A., Koseki T. Slip band formation at free surface of lath martensite in low carbon steel. *Acta Materialia*. 2019;165:129–141. <https://doi.org/10.1016/j.actamat.2018.11.026>
- Chen T., Chiba T., Koyama M., Shibata A., Akiyama E., Takai K. Hierarchical characteristics of hydrogen-assisted crack growth and microstructural strain evolution in tempered martensitic steels: Case of quasi-cleavage fracture. *Metallurgical and Materials Transactions A*. 2021;52(10):4703–4713. <https://doi.org/10.1007/s11661-021-06423-1>
- Krauss G., Marder A.R. The morphology of martensite in iron alloys. *Metallurgical Transactions*. 1971;2(9):2343–2357. <https://doi.org/10.1007/BF02814873>
- Morito S., Tanaka H., Konishi R., Furuhashi T., Maki T. The morphology and crystallography of lath martensite in Fe–C alloys. *Acta Materialia*. 2003;51(6):1789–1799. [https://doi.org/10.1016/S1359-6454\(02\)00577-3](https://doi.org/10.1016/S1359-6454(02)00577-3)
- Teplyakova L., Gershteyn G., Popova N., Kozlov E., Ignatenko L., Springer R., Schaper M., Bach Fr.-W. Scale-dependent hierarchy of structural elements in the microstructure of thermomechanical treated ferritic steels with residual austenite. *Materialwissenschaft und Werkstofftechnik*. 2009;40(9):704–712. <https://doi.org/10.1002/mawe.200900503>
- Morsdorf L., Jeannin O., Barbier D., Mitsuhara M., Raabe D., Tazan C.C. Multiple mechanisms of lath martensite plasticity. *Acta Materialia*. 2016;121:202–214. <https://doi.org/10.1016/j.actamat.2016.09.006>
- Teplyakova L.A., Popova N.A., Kozlov E.V. Localization of plastic deformation in tempered martensitic steels at large-scale levels. *Fundamental'nye problemy sovremennoy materialovedeniya (Basic Problems of Material Science (BPMS))*. 2012;9(4-2):659–663. (In Russ.).
Теплякова Л.А., Попова Н.А., Козлов Э.В. Локализация пластической деформации в отпущенных мартенситных сталях на крупномасштабных уровнях. *Фундаментальные проблемы современного материаловедения*. 2012;9(4-2):659–663.
- Teplyakova L.A., Popova N.A., Kunitsyna T.S. Localization of deformation in martensitic steels at the struc-

tural and scale level: Grain. Bands of localized deformation. *Fundamental'nye problemy sovremennogo materialovedeniya (Basic Problems of Material Science (BPMS))*. 2018;15(4):331–338. (In Russ.).

Теплякова Л.А., Попова Н.А., Куницына Т.С. Локализация деформации в мартенситных сталях на структурно-масштабном уровне: зерно. Полосы локализованной деформации. *Фундаментальные проблемы современного материаловедения*. 2018;15(4):331–338.

15. Teplyakova L.A., Kashin A.D., Kunitsyna T.S. Development of shear deformation in lath martensite of medium-alloy steels under tension. *Izvestiya. Ferrous Metallurgy*. 2023;66(2):154–161.
<https://doi.org/10.17073/0368-0797-2023-2-154-161>

Теплякова Л.А., Кашин А.Д., Куницына Т.С. Развитие сдвиговой деформации в пакетном мартенсите средне-легированных сталей при растяжении. *Известия вузов. Черная металлургия*. 2023;66(2):154–161.
<https://doi.org/10.17073/0368-0797-2023-2-154-161>

16. Kozlov E.V., Popova N.A., Ignatenko L.N., Grigorieva N.A., Kovalevskaya T.A., Teplyakova L.A., Chukhin B.D. Stages of plastic deformation, evolution of structure and sliding pattern in alloys with dispersed hardening. *Izvestiya vuzov. Physics*. 1991;34(3):112–128. (In Russ.).

Козлов Э.В., Попова Н.А., Игнатенко Л.Н., Григорьева Н.А., Ковалевская Т.А., Теплякова Л.А., Чухин Б.Д. Стадии пластической деформации, эволюция структуры и картина скольжения в сплавах с дисперсным упрочнением. *Известия вузов. Физика*. 1991;34(3):112–128.

17. Kozlov E.V., Popova N.A., Ignatenko L.N., Teplyakova L.A., Klopotov A.A. Patterns of substructural-phase transformations during plastic deformation of martensitic steel. *Izvestiya vuzov. Physics*. 1994;37(4):76–82. (In Russ.).

Козлов Э.В., Попова Н.А., Игнатенко Л.Н., Теплякова Л.А., Клопотов А.А. Закономерности субструктурно-фазовых превращений при пластической деформации мартенситной стали. *Известия вузов. Физика*. 1994;37(4):76–82.

18. Abdollah-Zadeh A., Jafari-Pirlari A., Barzegari M. Tempered martensite embrittlement in a 32NiCrMoV125 steel. *Journal of Materials Engineering and Performance*. 2005;14(5):569–573. <https://doi.org/10.1361/105994905X64657>

19. Du C., Hoefnagels J.P.M., Vaes R., Geers M.G.D. Plasticity of lath martensite by sliding of substructure boundaries. *Scripta Materialia*. 2016;120:37–40.
<https://doi.org/10.1016/j.scriptamat.2016.04.006>

20. Kadkhodapour J., Butz A., Ziaei-Rad S., Schmauder S. A micro mechanical study on failure initiation of dual tension using single crystal plasticity model. *International Journal of Plasticity*. 2011;27(7):1103–1125.
<https://doi.org/10.1016/j.ijplas.2010.12.001>

21. Shibata A., Gutierrez-Urrutia I., Nakamura A., Okada K., Miyamoto G., Madi Y., Besson J., Hara T., Tsuzaki K. Three-dimensional propagation behavior of hydrogen-related intergranular cracks in high strength martensitic steel. *International Journal of Hydrogen Energy*. 2023;48(88):34565–34574.
<https://doi.org/10.1016/j.ijhydene.2023.05.211>

22. Li S., Zhu G., Kang Y. Effect of substructure on mechanical properties and fracture behavior of lath martensite in 0.1C–1.1Si–1.7Mn steel. *Journal of Alloys and Compounds*. 2016;675:104–115.
<https://doi.org/10.1016/j.jallcom.2016.03.100>

23. Trishkina L.I., Klopotov A.A., Potekaev A.I., Cherkasova T.V., Borodin V.I., Kulagina V.V. Regularities of micro-crack propagation in substructures. *Russian Physics Journal*. 2023;66(1):416–430.
<https://doi.org/10.1007/s11182-023-02956-7>

24. Kozlov E.V., Teplyakova L.A., Popova N.A., Ignatenko L.N., Klopotov A.A., Koneva N.A. Influence of substructure type on carbon redistribution in martensitic steel during plastic deformation. *Izvestiya vuzov. Physics*. 2002;45(3):72–86. (In Russ.).

Козлов Э.В., Теплякова Л.А., Попова Н.А., Игнатенко Л.Н., Клопотов А.А., Конева Н.А. Влияние типа субструктур на перераспределение углерода в стали мартенситного класса в ходе пластической деформации. *Известия вузов. Физика*. 2002;45(3):72–86.

Information about the Authors

Сведения об авторах

Lyudmila A. Teplyakova, Dr. Sci. (Phys.–Math.), Prof. of the Chair of Physics, Tomsk State University of Architecture and Building

ORCID: 0000-0001-5038-7379

E-mail: lat168@mail.ru

Tat'yana S. Kunitsyna, Cand. Sci. (Phys.–Math.), Assist. Prof. of the Chair of Advanced Mathematics, Tomsk State University of Architecture and Building

ORCID: 0000-0001-6801-4909

E-mail: kma11061990@mail.ru

Vladislav A. Pechkovskii, Postgraduate, Tomsk State University of Architecture and Building

E-mail: Poits16@yandex.ru

Aleksandr D. Kashin, Postgraduate, Institute of Strength Physics and Materials Science, Siberian Branch of Russian Academy of Sciences

ORCID: 0000-0003-1860-3654

E-mail: kash@mail.ru

Людмила Алексеевна Теплякова, д.ф.-м.н., профессор кафедры физики, Томский государственный архитектурно-строительный университет

ORCID: 0000-0001-5038-7379

E-mail: lat168@mail.ru

Татьяна Семеновна Куницына, к.ф.-м.н., доцент кафедры высшей математики, Томский государственный архитектурно-строительный университет

ORCID: 0000-0001-6801-4909

E-mail: kma11061990@mail.ru

Владислав Андреевич Печковский, аспирант, Томский государственный архитектурно-строительный университет

E-mail: Poits16@yandex.ru

Александр Данилович Кашин, аспирант, Институт физики прочности и материаловедения СО РАН

ORCID: 0000-0003-1860-3654

E-mail: kash@mail.ru

Contribution of the Authors

Вклад авторов

L. A. Teplyakova – problem statement, analysis of research results, formulation of conclusions.

T. S. Kunitsyna – complex metallographic and electron microscopic analysis.

V. A. Pechkovskii – measurement of quantitative characteristics of deformation relief.

A. D. Kashin – statistical processing of the data obtained.

Л. А. Теплякова – постановка задачи, анализ результатов исследований, формулировка выводов.

Т. С. Куницына – комплексное металлографическое и электронно-микроскопическое исследование.

В. А. Печковский – измерение количественных характеристик деформационного рельефа

А. Д. Кашин – статистическая обработка полученных данных.

Received 20.09.2024

Revised 23.10.2024

Accepted 17.12.2024

Поступила в редакцию 20.09.2024

После доработки 23.10.2024

Принята к публикации 17.12.2024